

## Ash Characteristics and Hot-Gas Filter Performance at the PSDF

Robert S. Dahlin ([rsdahlin@southernco.com](mailto:rsdahlin@southernco.com); 205-670-5068)  
E. Carl Landham ([eclandha@southernco.com](mailto:eclandha@southernco.com); 205-670-5990)  
Southern Research Institute  
Power Systems Development Facility  
P. O. Box 1069  
Wilsonville, AL 35186

Howard L. Hendrix ([hlhendri@southernco.com](mailto:hlhendri@southernco.com); 205-670-5876)  
Southern Company Services  
Power Systems Development Facility  
P. O. Box 1069  
Wilsonville, AL 35186

### Background And Objectives

Previous evaluations of ceramic candle filters have shown that filter performance and reliability can be highly dependent on the characteristics of the ash that is being collected. Changes in ash particle size, morphology, and chemistry can have profound effects on dustcake permeability and filter pressure drop. In some cases, undesirable ash characteristics have led to the accumulation of tenacious deposits within the filter system that have been responsible for the failure of filter elements. It is becoming increasingly clear that successful design and operation of hot-gas filter systems must be based on an understanding of the particulate characteristics that influence dustcake permeability and that cause accumulation of tenacious deposits. Consequently, the understanding of particulate characteristics is considered a cornerstone of the filter test program at the Power Systems Development Facility (PSDF).

A realistic understanding of particulate characteristics is fundamentally dependent upon the collection of particulate samples that are representative in terms of their mass concentration, particle-size distribution, chemical composition, and other physical properties. To provide the particulate samples needed to assess filter performance, Southern Research Institute has designed and is now operating sampling systems for collecting representative samples of the particulate matter entering and leaving the hot-gas filter. These sampling systems represent a significant improvement over the extractive sampling systems that have been used to collect particulate samples from high-temperature, high-pressure gas streams at other test facilities (Farthing and Yue, 1991). It has been shown that particles suspended in extractive sampling lines can be deposited in the lines and subsequently reentrained as larger agglomerates, thereby altering the particle-size distribution (Anand et al, 1992). Further alteration of the particulate properties is possible by condensation of alkali vapors and other condensibles, because it is usually very difficult to maintain extractive sampling lines at process temperature. Because of these potential problems, the particulate sampling systems used at the PSDF have been designed to collect the particles in a sampler that is inserted directly into the process gas stream. This *in-situ* approach

ensures that the sample is collected under actual process conditions, and the sample is not lost or altered during sample collection, making it possible to accurately quantify the loadings and particle-size distributions of the solids suspended in the flue gas.

## **Particulate Sampling Systems**

The key elements of the *in-situ* particulate sampling systems are illustrated in Figure 1. Bulk particulate samples can be collected in a single-filter sampler, or size-segregated samples can be collected in a cascade impactor. A high-temperature cyclone assembly is also being developed to provide larger, size segregated samples. The sampling probe, which will accept any one of these samplers, comprises an inner tube through which the particulate-free sample gas flows and a coaxial outer tube that supports the sampler and provides the rigidity required for insertion into the high-pressure process stream. The sample gas exiting the probe is cooled to remove condensibles and metered through a calibrated flow orifice to ensure that samples are collected isokinetically. On-line access to the process gas stream is provided by a set of double-block-and-bleed valves, which are equipped with nitrogen purge to minimize buildup of dust and process gas in the casing. The sampling probe is inserted and retracted using a motorized screw mechanism with a built-in encoder and computer control system to ensure accurate positioning of the sampler. More detailed descriptions of the sampling system design and operation have been published elsewhere (Dahlin et al, 1993, 1995, and 1997).

Since their initial use in October 1996, the *in-situ* particulate sampling systems have operated very reliably with nearly 100% availability. The systems have been proven to be capable of detecting particulate loadings as low as 0.5 ppmw. Errors introduced by gas-substrate interactions and by substrate handling have been equivalent to less than 0.2 ppmw. The only significant operational problem has been chloride pitting corrosion in the condensate collection system, which has been addressed by changing these components to Hastelloy C-276.

## **Particulate Loadings And Filter Collection Efficiency**

Particulate sampling runs have been performed on a regular basis during all of the major PSDF test campaigns. These sampling runs have been primarily directed at monitoring changes in solids carryover from the Transport Reactor system and at detecting any particle penetration that might be associated with the failure of one or more filter elements. A summary of the total particulate loadings measured at the hot-gas filter inlet is given in Figure 2. Inlet particulate loadings were initially high as a result of frequent upsets in the dipleg seal on the Primary Cyclone of the Transport Reactor system. The dipleg upsets caused large slugs of solids to be carried over to the hot-gas filter, producing loadings as high as 100,000 ppmw. Various improvements in Transport Reactor operating procedures have greatly reduced the magnitude and frequency of the dipleg upsets, resulting in more stable inlet loadings. During the last major test campaign (TC01), the mean inlet loading was 11,400 ppmw  $\pm$  2,300 ppmw (20% relative standard deviation).

Figure 3 summarizes the outlet particulate loadings measured during TC01. Prior to the first TC01 outlet sampling run on September 9, it had already been determined that one filter element

had been broken. Even with one broken filter element, the measurements performed during the period of September 9 to September 19 showed that the outlet loading was still quite low (0.10 ppmw to 0.53 ppmw), suggesting that the failsafe device on the broken element prevented high levels of particle penetration during this initial time period. On September 19, it was determined that one additional element had broken, and measurements made between September 19 and October 31 showed that the outlet loading had increased significantly, with the measured values ranging from 3.8 ppmw to about 13 ppmw. This result suggested that the failsafe device on the broken element was not working properly, or that some other leak had developed that was allowing ash particles to penetrate from the dirty side to the clean side of the filter.

On November 2, a severe thermal excursion occurred when problems were encountered with the coal feed to the Transport Reactor system. While operations personnel were trying to reestablish stable coal feed, the ash discharge system became plugged with a large number of ceramic fragments, forcing a shutdown of the Transport Reactor system. Subsequent inspection of the filter internals revealed that a total of 13 filter elements had been broken. The broken elements were replaced, and the system was restarted on November 19, although stable operation on coal was not achieved for several days. The outlet particulate measurements made between December 1 and 8 indicated that the outlet loading was still in the range of 3.9 ppmw to 5.3 ppmw, suggesting that there was still some sort of leak from the dirty side to the clean side of the filter. Subsequent inspection of the filter internals revealed that all of the elements appeared to be intact, and a pressure test failed to detect any leaks in the filter plenums, suggesting that the particle penetration was probably occurring through leaking gaskets between the filter elements and the tubesheet.

Although the outlet loadings measured after September 19 were higher than expected, it is important to note that the outlet loading never exceeded 13 ppmw. Based on the average inlet loading of 11,400 ppmw, this outlet loading would correspond to a minimum collection efficiency of 99.89%. As illustrated in Figure 4, the collection efficiencies calculated on this basis exceeded 99.99% prior to September 19. After that date, efficiency values ranged from 99.89 to 99.97%. Thus, even the lowest collection efficiency recorded during TC01 was still quite good compared to the performance of most particulate control systems that are currently operating on coal-fired power plants.

## **Particle-Size Distributions**

Figure 5 shows particle-size distributions measured on various inlet particulate samples on the basis of cumulative percentage of the mass contained in particles smaller than a given size. Figure 6 shows the same particle-size data presented as a differential mass distribution (i.e., the particulate mass contained in a given particle-size increment). The inlet size distributions show a general progression toward finer particle sizes consistent with the trend in particulate loadings, both of which reflect the reduction in solids carryover that was achieved by better control of cyclone dipleg upsets. Comparison of the differential mass distributions (Figure 6) shows that the distinct, large-particle mode that was evident in the early (CCT4) data was eliminated in the subsequent tests. Chemical analysis of the samples confirmed that the CCT4 samples contained more sand than the samples from the other test campaigns, suggesting that the large-particle

mode in the CCT4 samples resulted from carryover of bed material.

Prior to the development of leaks through the filter element gaskets or failsafes, the mass concentration at the PCD outlet was too low to make accurate particle-size distribution measurements. However, after the increase in emissions on September 9, the outlet size distribution could be effectively measured. Figure 7 shows a comparison of the average inlet and outlet particle-size distributions measured during this high-emissions period of TC01. These measurements indicate that the ash penetrating through the leaks is much finer ( $mmd \cong 2 \mu m$ ) than the dust entering the PCD. Nevertheless, it appears that some of the particles that were leaking to the outlet may be large enough to be of concern from the standpoint of turbine blade erosion, since particles larger than  $5 \mu m$  account for approximately 20% of the total particulate mass, or about 1.3 ppmw. These results highlight the importance of effective gasketing and failsafe systems for maintenance of lowest emissions and maximum turbine protection.

## Particulate Chemistry

Chemical analyses are performed routinely on samples taken from the filter hopper, samples taken from the filter dustcake, and samples collected in the *in-situ* particulate sampling systems. Based on the analyses of TC01 samples, the average calcium utilization (i.e., the percentage of the calcium that is converted to calcium sulfate on a molar basis) was  $44.6\% \pm 8.9\%$ . Given the large standard deviation, this value of utilization is indistinguishable from the 50% utilization that we would expect based on the observed  $SO_2$  removal (essentially 100%) and the targeted injection rate of dolomite (2:1 calcium-to-sulfur ratio, nominally). Since the sorbent is dolomite, and the inherent calcium in the coal is quite low (typically  $<1\%$  of the coal ash), we would expect the calcium-to-magnesium molar ratio in the ash to be close to 1:1. The average calcium-to-magnesium ratio calculated from the chemical analyses is 0.98:1, providing some reassurance that the analyses are reliable.

The chemical analyses have been used to calculate the average chemical composition of the solids samples, assuming that all of the sulfur is present as  $CaSO_4$  and all of the carbonate is present as  $CaCO_3$ . Any remaining calcium that is not accounted for as  $CaSO_4$  or  $CaCO_3$  is assumed to be present as  $CaO \bullet MgO$ , and any remaining magnesium that is not accounted for as  $CaO \bullet MgO$  is assumed to be present as  $MgO$ . The balance of each sample is assumed to be ash and sand (bed material). The choice of these particular calcium and magnesium compounds was based on free-energy minimization calculations performed by Dr. L. Shadle at DOE/FETC (Smith, 1998). Some of the chemical compositions calculated in this manner are compared in Table 1.

As shown in Table 1, the November dustcake samples contain more  $CaSO_4$  and  $MgO$  and less  $CaCO_3$  and  $CaO \bullet MgO$  than do the January dustcake samples. This suggests that more of the  $CaO \bullet MgO$  has been converted to  $CaSO_4$  and  $MgO$  in the November dustcake samples. Although the concentration of  $CaSO_4$  in the November dustcake samples is similar to that found in the hopper samples, the concentration of  $CaO \bullet MgO$  is significantly lower in both sets of dustcake samples than it is in the hopper samples ( $3.11 \pm 0.61\%$  versus  $9.06 \pm 2.48\%$ ). The relatively low levels of  $CaO \bullet MgO$  in the November dustcake samples, coupled with  $CaSO_4$

levels that are comparable to those of the hopper samples, result in a significantly higher calcium utilization in the November dustcake samples (65 to 73% versus 34 to 53% for the hopper samples and the January dustcake samples).

In attempting to understand these compositional differences between the dustcake samples and the other types of samples, it is important to note that the dustcake samples represent residual solids that are left on the candles after numerous process transients, including several system startups, shutdowns, disruptions in coal and sorbent feed, and numerous back-pulses after shutdown. Also, it is possible that the larger particles in the inlet gas stream are not collected on the filter elements in representative numbers. Therefore, it is not surprising that the chemical composition of the ash samples taken from the filter elements after shutdown is different from that of the ash samples taken from the filter hopper during testing. Additional work will be required to develop a better understanding of the factors that determine the ultimate chemical composition of the residual dustcake.

### **Permeability and Other Physical Properties**

Table 2 summarizes the results of permeability tests and other physical measurements performed on in-situ samples, dustcake samples, and hopper samples. The permeability test results are expressed in terms of drag-equivalent diameter (DED), which is not a physical size, but rather a fitted parameter that can be used to rank the gas flow resistance of ashes at equal porosities. Measurements of physical size generally correlate with DED, but the DED best expresses the fineness of an ash as it relates to its effect on gas flow resistance (drag). Increasing values of DED indicate lower resistance to gas flow (less drag) at a given porosity. Using the DED as an indicator of flow resistance eliminates much of the ambiguity associated with drag measurements, which are a strong function of porosity.

In terms of the physical properties given in Table 2, the in-situ samples appear to be fairly similar to the hopper samples, but there appears to be some significant differences between these types of samples and the dustcake samples. The true densities, bulk densities, and uncompacted bulk porosities of the dustcake samples are similar to the values measured for the other samples. However, the dustcake samples exhibit somewhat higher surface areas along with lower mass-median diameters, DEDs, and calcium content. The mathematical models that are currently being used to correlate drag data predict that a smaller mass-median diameter or a higher surface area would tend to produce a smaller DED (i.e., more drag).

Figure 8 shows the results of permeability (drag) measurements on the two dustcake samples that were discussed in the previous section on particulate chemistry. The substantial difference in the flow resistance between the November and January dustcake samples suggests that there is a substantial difference in the physical characteristics of these two dustcakes. One such difference is evident in the particle-size distributions shown in Figure 9. Comparison of the size distributions reveals that the November sample contains a significantly higher concentration of particles smaller than 4  $\mu\text{m}$  than does the January sample. This difference could at least partly account for the observed difference in flow resistance. Other differences between the two samples are summarized in Table 3.

The differences in uncompacted bulk porosity, specific surface area, mass-median diameter, and drag-equivalent diameter are most probably a direct result of the difference in particle-size distribution. The difference in particle-size distribution could be related to the differences in chemical composition discussed earlier. Sorbent-related compounds account for about 20 to 21% of the material in the November sample and only about 12 to 15% of the material in the January sample. This result suggests that the carryover of dolomite to the filter was higher during the pre-November portion of TC01 than it was afterwards. The last hopper sample collected before the November inspection contained 8.65% calcium and 3.09% sulfur, and the calcium-to-sulfur molar ratio was 2.24:1. The last hopper sample collected before the January inspection contained 7.71% calcium and 2.86% sulfur, and the calcium-to-sulfur molar ratio was 2.16:1. Thus, the hopper samples also suggest that more dolomite was entering the filter during the pre-November portion of TC01 than during the pre-January portion.

### **Dustcake Drag And Filter Pressure Drop**

Based on measurements made during the January PCD inspection, the average areal loading of the residual dustcake was determined to be  $0.47 \text{ lb/ft}^2$ , and the average porosity of the residual dustcake was determined to be 76%. (Note that this value of porosity is substantially lower than the uncompacted bulk porosity given in Table 3, suggesting that the dustcake has been compressed significantly by the compressive force exerted by the filter pressure drop. This compression has been observed in laboratory permeability and compressibility tests.) From Figure 8, the normalized dustcake drag at a porosity of 76% and at room temperature is about  $11 \text{ in.wc}/(\text{ft}/\text{min})/(\text{lb}/\text{ft}^2)$ . To calculate the actual drag on the residual cake during operation, this value of normalized drag, which was measured in the laboratory, must be corrected to filter conditions by multiplying by the ratio of the flue gas viscosity at process conditions ( $\approx 400 \mu\text{P}$ ) to the viscosity of air at room temperature ( $\approx 180 \mu\text{P}$ ). The dustcake drag predicted in this manner is  $24 \text{ in.wc}/(\text{ft}/\text{min})/(\text{lb}/\text{ft}^2)$  at process conditions. This value of residual dustcake drag would apply to the stable operating period immediately prior to the January shutdown, when the average filter face velocity was  $4.6 \text{ ft}/\text{min}$ .

Based on a residual dustcake areal loading of  $0.47 \text{ lb}/\text{ft}^2$ , a face velocity of  $4.6 \text{ ft}/\text{min}$ , and a drag of  $24 \text{ in.wc}/(\text{ft}/\text{min})/(\text{lb}/\text{ft}^2)$ , the pressure drop across the residual dustcake is calculated to be  $52 \text{ in.wc}$ . To calculate the corresponding baseline pressure drop across the entire filter system, this pressure drop across the residual dustcake must be combined with the pressure drop across the filter elements themselves and the other pressure losses associated with flow through the filter vessel internals. The pressure drop attributable to the filter elements and vessel internals may be inferred from the observed pressure drop during a system startup on propane in the absence of solids carryover to the filter, which is about  $18 \text{ in.wc}$  when corrected for the effect of gas viscosity. Adding these pressure losses to the predicted pressure drop across the residual dustcake yields a predicted baseline pressure drop of  $70 \text{ in.wc}$ , which is in reasonably good agreement with the baseline pressure drop observed during the pre-January portion of TC01 operations ( $\approx 75 \text{ in.wc}$ ). Thus, assuming that the measured areal loading and porosity of the residual dustcake are correct, this calculation suggests that the laboratory measurement of residual dustcake drag is consistent with the baseline pressure drop observed during the pre-January portion of TC01 operations.

The calculations summarized above will be repeated as additional information on residual dustcake characteristics becomes available from future tests. Current plans call for ending the next test campaign (TC02) with a “dirty shutdown” of the filter, in which coal flow to the transport reactor will be stopped near the end of a 40-min. filtration cycle with no additional back-pulses. The dirty shutdown will make it possible to obtain samples of the entire dustcake, so that we can further check the consistency between laboratory drag measurements and observed filter pressure drop.

## **Summary and Conclusions**

When all filter elements are intact and properly gasketed, the collection efficiency of the hot-gas filter at the PSDF has been 99.99% or higher. In cases where filter elements were broken or leakage occurred through gaskets, collection efficiencies as low as 99.89% have been measured, corresponding to outlet loadings as high as 13 ppmw. Thus, even the lowest collection efficiencies recorded to date have been quite good compared to the performance of most particulate control systems that are currently operating on coal-fired power plants.

Permeability and particle-size measurements made on filter dustcakes suggest that the flow resistance of the dustcake increases with an increasing concentration of fine particles in the cake. The flow resistance of dustcake samples collected in November 1997 was more than double the flow resistance of dustcake samples collected in January 1998, and the November dustcake samples contained over twice the mass concentration of fine particles ( $D_p < 4 \mu\text{m}$ ). Chemical analyses suggest that the increased concentration of fine particles in the November dustcake may be associated with an increased level of sorbent-related compounds in the cake.

The porosity of the residual dustcake, which is a critical factor in determining filter permeance, appears to be substantially less than the uncompacted bulk porosity, suggesting that the dustcakes compress under loads comparable to the filter pressure drop. This compression has been observed in laboratory permeability and compressibility tests.

## Future Activities

Tests performed to date have identified several key questions that need to be addressed in future work.

- To what extent is the size distribution of the particulate matter entering the hot-gas filter system modified before it reaches the filter elements?
- What is the porosity of the dustcake during filter operation and how does it vary with dustcake thickness and with time in the filtration cycle?
- What are the relative contributions of system startup, transition to coal, and steady-state operations on the ultimate nature of the residual dustcake?
- How sensitive are particulate characteristics and filter performance to changes in coal and sorbent feedstocks?

The question of size-segregation in the filter vessel is being addressed through a series of tests in which we will separately collect the ash that drops out between back-pulses. These tests will be coordinated with inlet sampling runs so that we can compare the size distribution of the inlet ash to that of the ash that drop outs prior to collection on the filter elements. The question of dustcake porosity will be addressed by performing a “dirty shutdown” at the end of TC02. Coal flow to the Transport Reactor will be shut off near the end of a 40-min. filtration cycle, and the filter will not be subsequently pulsed to preserve the full (residual-plus-transient) dustcake. Analysis of the dustcake will provide valuable information on cake porosity, flow resistance, and other properties. Future sampling runs will include the collection of inlet samples during system startup (circulation of hot bed material) and during the transition to coal combustion. These samples will help us understand the nature and composition of the solids that initially form the residual dustcake. Comparison to the residual dustcake removed after the run may provide some insight into the influence of startup conditions on the ultimate character of the residual dustcake.

After TC02 is completed, the next run (TC03) will be done with the design coal and sorbent for the Lakeland Project. This testing will continue the exposure of some filter elements that are currently in use to ultimately reach the design life-cycle exposure expected at Lakeland. This testing should also help us identify any potential problems with ash deposition or dustcake flow resistance that might be associated with the Lakeland coal and sorbent. Following the completion of TC03, shakedown testing will begin on the Foster Wheeler APFBC system in first-generation configuration (combustor only). This testing will include commissioning the particulate sampling systems at the inlet and outlet of the hot-gas filter. Other future activities will include: demonstration of the particulate sampling systems on the Transport Reactor train in gasification mode; development and demonstration of a high-temperature cyclone assembly for collection of larger, size-segregated particulate samples; and demonstration of a real-time particulate monitor for detecting filter leakage.

## Contract Information

This work is being sponsored by the U.S. Department of Energy's Federal Energy Technology Center under Contract DE-FC21-90MC25140 with Southern Company Services, P. O. Box 1069, Wilsonville, AL 35186, Fax: 205-670-5843.

## Acknowledgments

The authors gratefully acknowledge the guidance of the FETC Contracting Officer's Representative, Mr. James Longanbach; the PSDF Plant Manager, Mr. Randall Rush; the PSDF Technical Manager, Mr. Tim Pinkston; and other members of the PSDF hot-gas filter team: Matt Davidson, Edwin Galloway, Xiaofeng Guan, and Patrick Scarborough. Operation and maintenance of the particulate sampling systems is provided by SRI's on-site sampling technicians, Terry Hammond and Sadler Sanders. Members of SRI's sampling system design team included: Jim Wright (Mechanical), Bill Steele (Instrumentation and Controls), Tom McGuire (CAD), and Bill Farthing (Aerosol Sampling). The SRI Project Manager is Dr. Duane Pontius. Pete Smith of M. W. Kellogg and Larry Shadle of FETC developed the procedures used to calculate chemical compositions of the PSDF solids. Zal Sanjana and Eugene Smeltzer of Westinghouse contributed many valuable comments on the results of the hot-gas filter testing and plans for future tests at the PSDF. Todd Snyder of SRI provided the measurements of dustcake porosity.

## References

- Anand, N. K., A. R. McFarland, K. D. Kihm, and F. S. Wong. "Optimization of Aerosol Penetration Through Transport Lines." *Aerosol Sci Technol.* Vol. 16, No. 2, p. 105 (1992).
- Dahlin, R. S., W. E. Farthing, and D. H. Pontius. "In-Situ Particulate Sampling System for Evaluating Control Devices at High Temperature and at High Pressure." Paper presented at the Tenth Particulate Control Symposium. Washington, DC. April 5-8, 1993.
- Dahlin, R. S., D. H. Pontius, Z. U. Haq, P. Vimalchand, R. Brown, and J. Wheeldon. "Plans for Hot Gas Cleanup Testing at the Power Systems Development Facility." Proceedings of the 13<sup>th</sup> International Conference on Fluidized-Bed Combustion. Vol. 1, p.449 (1995).
- Dahlin, R. S., E. C. Landham, and H. L. Hendrix. "In-Situ Particulate Sampling and Characterization at the Power Systems Development Facility." Paper presented at the Sixteenth Annual Conference of the American Association for Aerosol Research. Denver, Colorado. October 13-17, 1997.
- Farthing, W. E. and P. S. Yue. "Particulate Characterization from a Sub-Pilot-Scale Entrained-Bed Gasifier." Paper presented at the Ninth Particulate Control Symposium. Williamsburg, Virginia. October 15-18, 1991.
- Smith, P. V. Personal Communication to R. S. Dahlin. March 6, 1998.

**Table 1. Chemical Composition of Dustcakes and and Hopper Ash Samples**

	Dustcake - 11/5/97	Dustcake - 1/21/98	Hopper Average
CaCO <sub>3</sub> , wt%	0.61 – 0.95	1.13 – 1.21	1.19 ± 0.45
CaSO <sub>4</sub> , wt%	10.29 – 11.77	3.61 – 5.99	11.33 ± 2.04
CaO•MgO, wt%	2.41 – 3.04	3.10 – 3.90	9.06 ± 2.48
MgO, wt%	5.70 – 6.11	2.83 – 3.73	3.94 ± 0.84
Ash/Sand (diff), wt%	79.10 – 80.02	85.97 – 88.54	74.48 ± 3.01

**Table 2. Properties of In-Situ Samples, Dustcake, and Hopper Samples**

	In-Situ	Dustcake	Hopper
True Density, g/cc	2.71 ± 0.13	2.80 ± 0.31	2.67 ± 0.04
Bulk Density, g/cc	0.54 ± 0.05	0.50 ± 0.02	0.59 ± 0.05
Uncompacted bulk porosity, %	79.8 ± 2.3	82.0 ± 2.0	77.1 ± 1.5
Surface Area, m <sup>2</sup> /g	2.96 ± 0.38	4.27 ± 0.63	N. D.
Mass-median diameter, μm	22.0 ± 3.7	8.7 ± 0.7	28.8 ± 9.7
Drag-equivalent diameter, μm	2.47 ± 0.62	1.68 ± 0.52	2.32 ± 0.57
Calcium content, wt %	8.17 ± 6.14	4.00 ± 0.80	8.05

**Table 3. Physical Properties of November and January Dustcakes**

Property	11/5/97 Dustcake	1/21/98 Dustcake
Uncompacted bulk porosity, %	83.3 to 83.9	80.5 to 81.3
Specific surface area, m <sup>2</sup> /g	4.71 to 5.03	3.64 to 3.88
Mass-median diameter, μm	8.0 to 8.8	9.5 to 9.8
Drag-equivalent diameter, μm	1.26 to 1.39	2.15 to 2.24
Calcium content, wt%	4.66 to 4.70	3.12 to 3.52
Sulfur content, wt%	2.42 to 2.77	0.85 to 1.41
Calcium-to-sulfur molar ratio	1.36 to 1.54	2.00 to 2.94

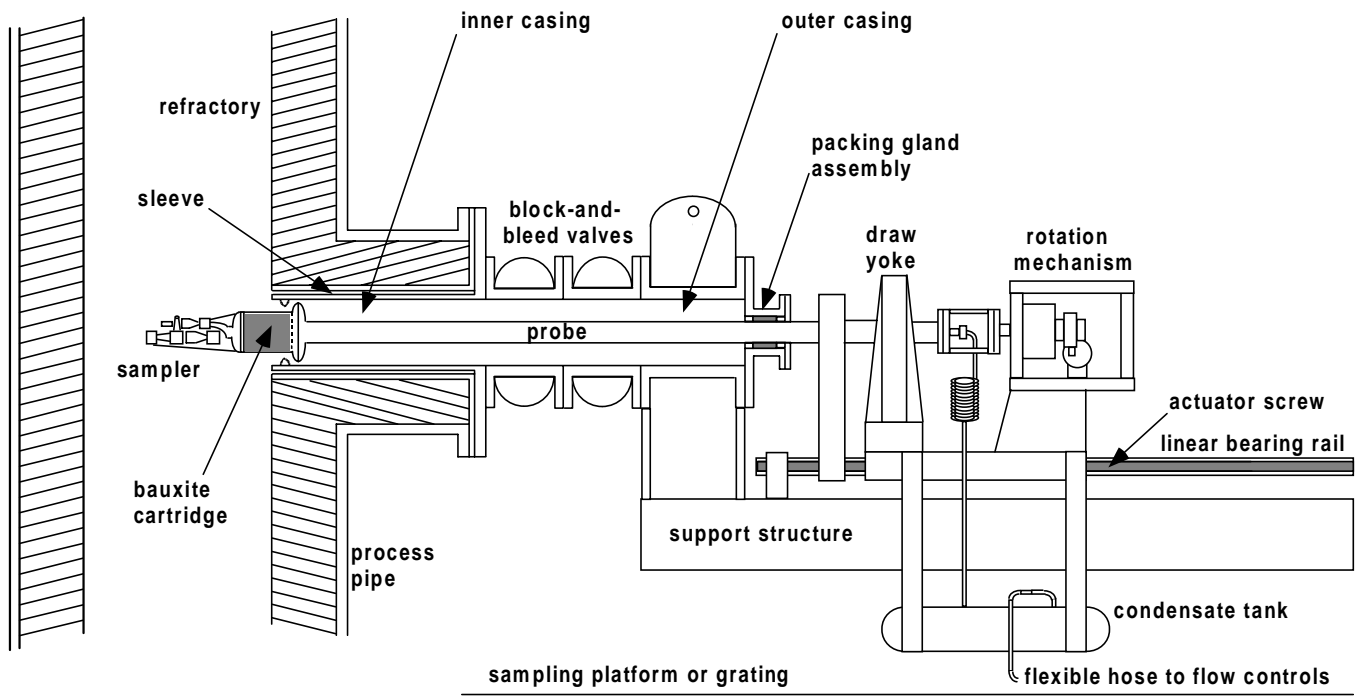


**Figure 1. General Arrangement of *In-Situ* Particulate Sampling System**

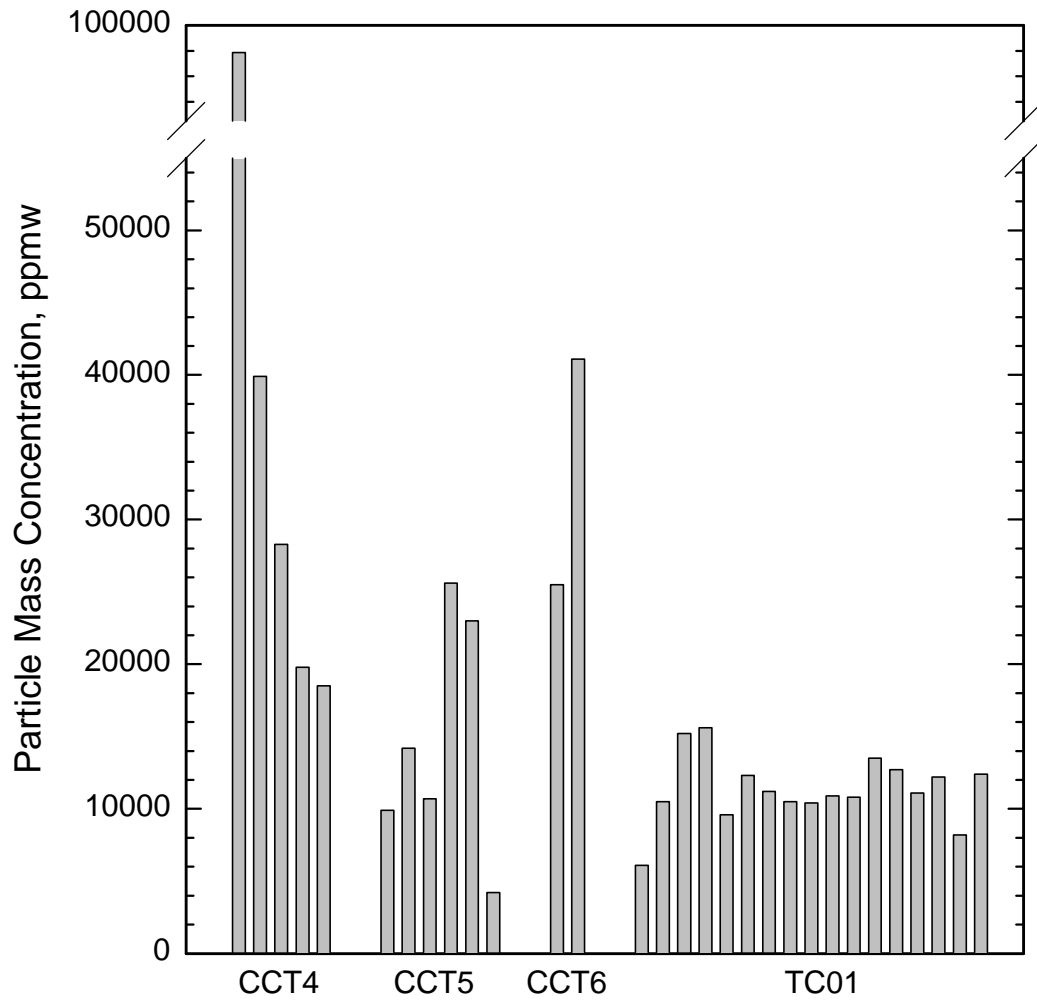


**Figure 2. Particulate Loadings Measured at Filter Inlet**

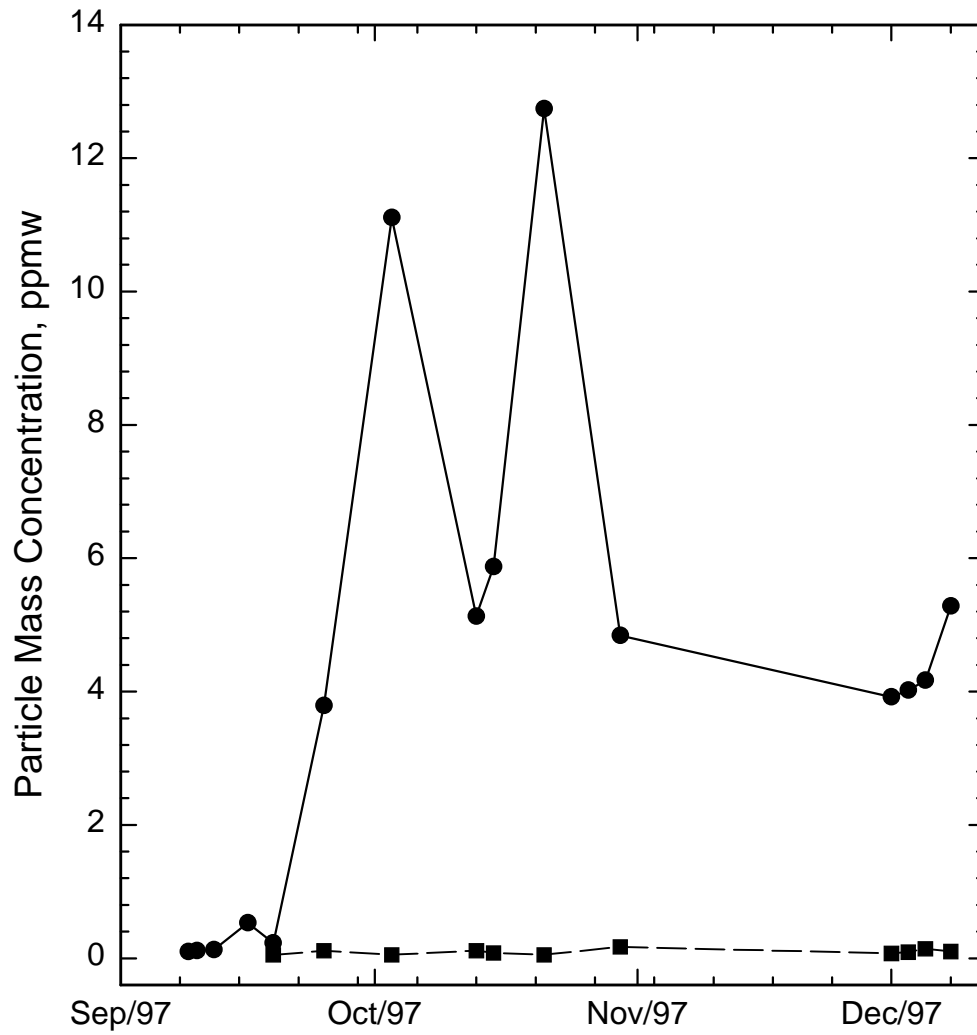


**Figure 3. Particulate Loadings Measured at Filter Outlet**

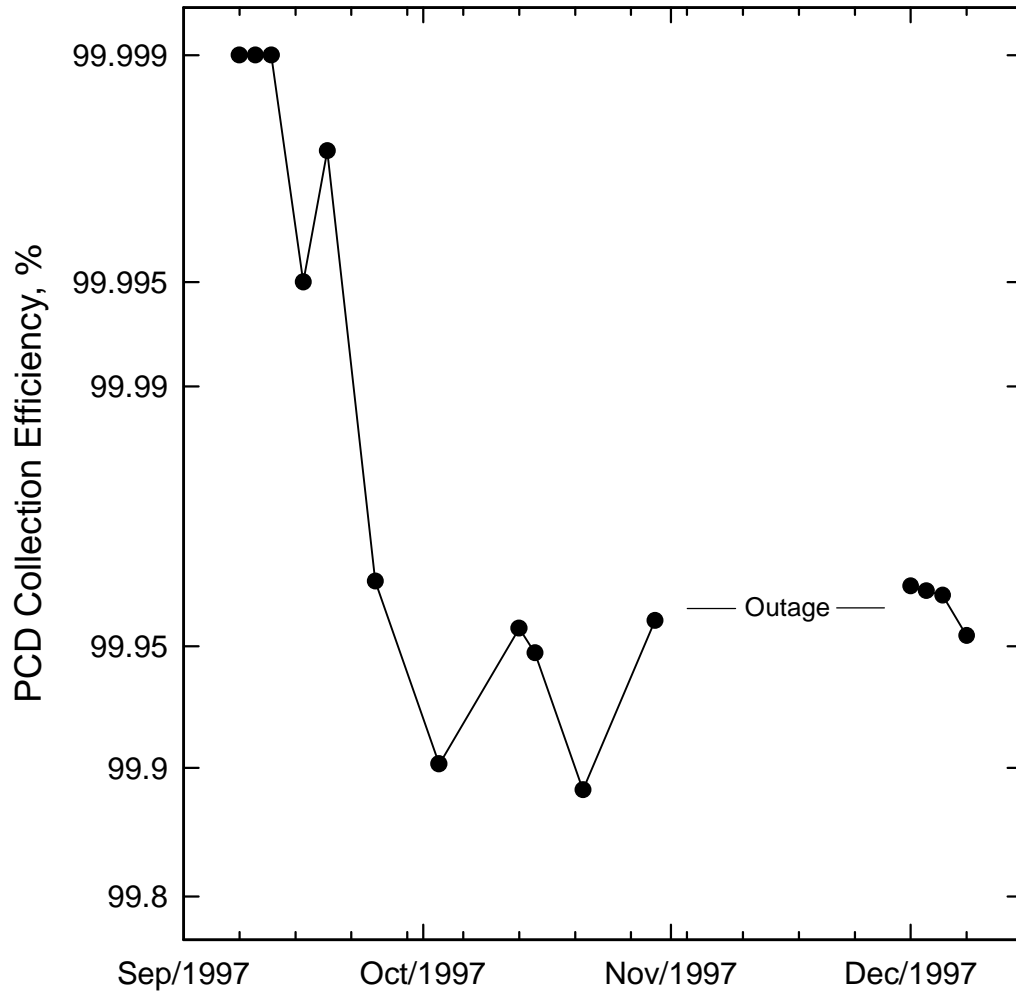


**Figure 4. Filter Collection Efficiencies**

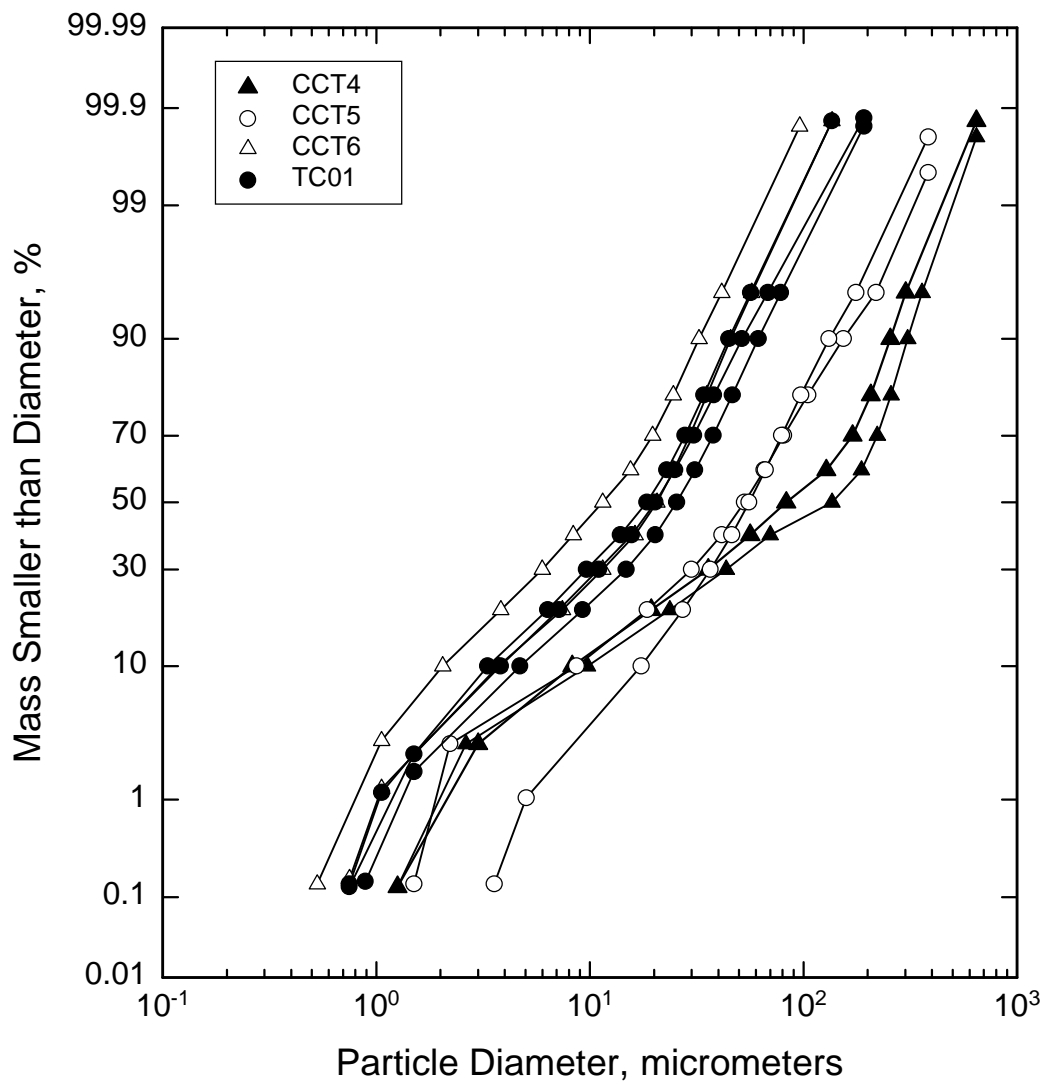


**Figure 5. Particle-Size Distributions Measured at Filter Inlet on a Cumulative Percentage Basis**

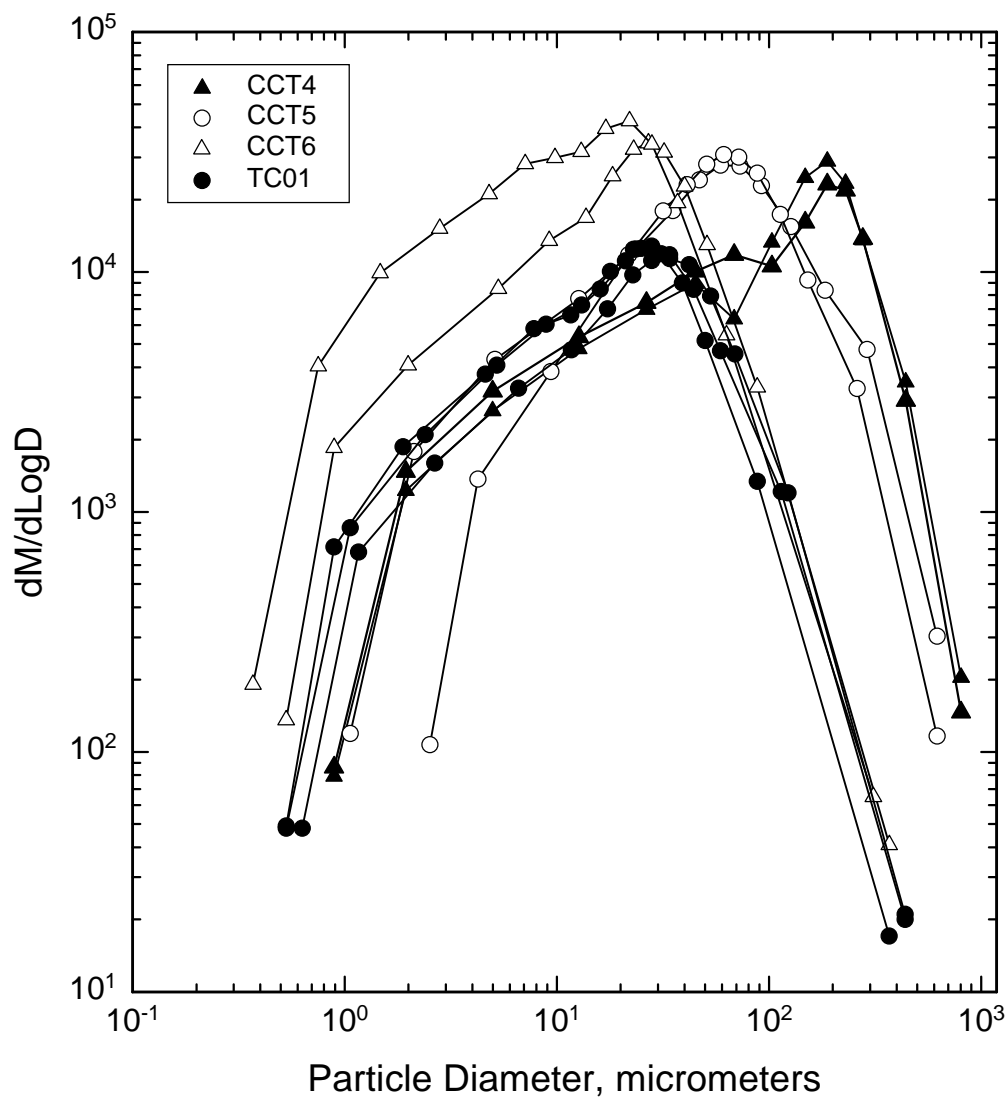


**Figure 6. Particle-Size Distributions Measured at PCD Inlet on a Differential Mass Basis**

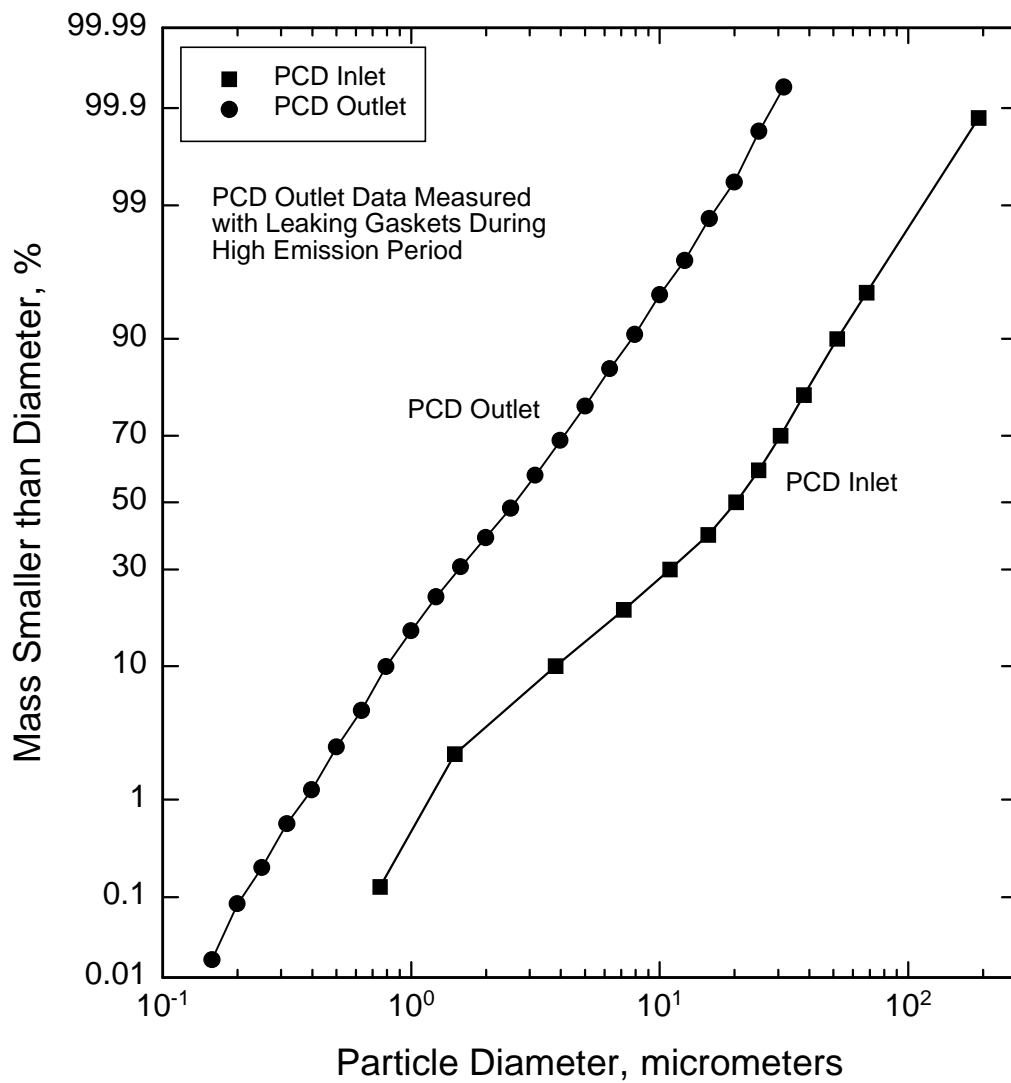


**Figure 7. Comparison of Inlet and Outlet Particle-Size Distributions**

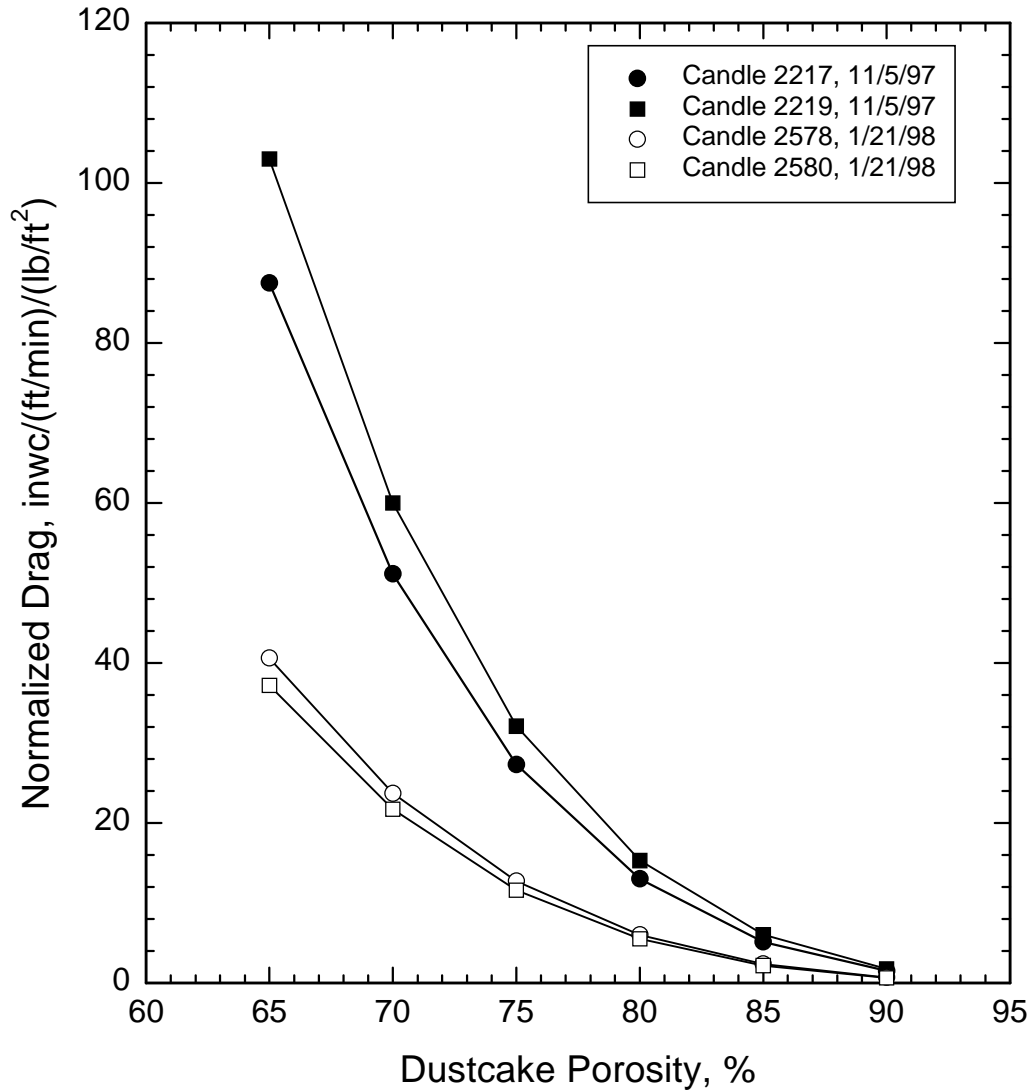


**Figure 8. Drag-Porosity Curves for November and January Dustcakes**

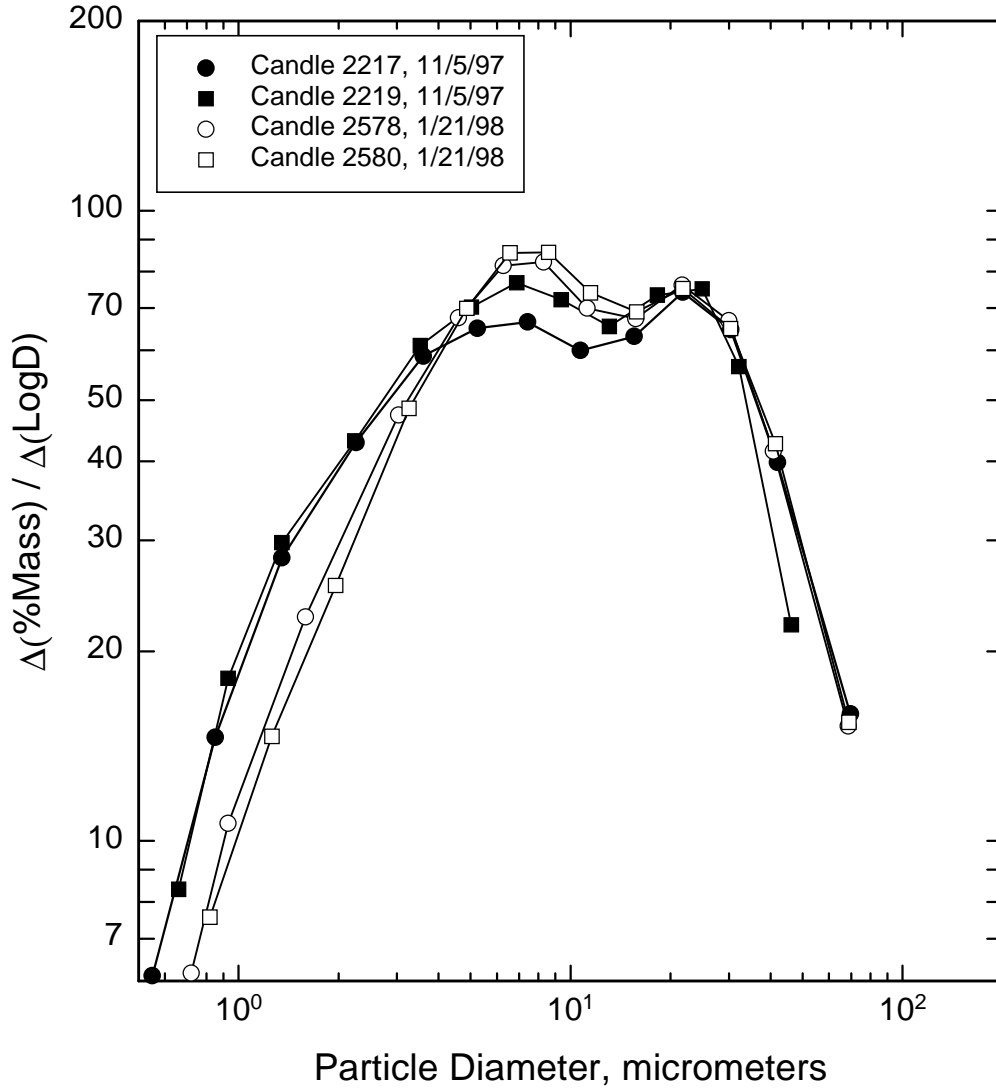


**Figure 9. Particle-Size Distributions of November and January Dustcakes**